

Surface changes in wood submitted to thermomechanical densification

Douglas Edson Carvalho¹ <https://orcid.org/0000-0002-2443-0510>^{*}

Márcio Pereira da Rocha² <https://orcid.org/0000-0002-5420-8478>

Ricardo Jorge Klitzke² <https://orcid.org/0000-0001-6839-9415>

Pedro Henrique Gonzalez de Cademartori² <https://orcid.org/0000-0003-3295-6907>

¹Universidade Federal do Sul da Bahia. Centro de Formação em Ciências Agroflorestais. Ilhéus, Bahia, Brasil.

²Universidade Federal do Paraná. Departamento de Engenharia e Tecnologia Florestal. Curitiba, Paraná, Brasil

^{*}Corresponding author: douglasedsoncarvalho@gmail.com

Abstract:

Ideal thermomechanical treatment conditions that reduce roughness and increase hydrophobicity of the wood surface require further investigation. In this study, a thermo-mechanical densification process was applied to *Gmelina arborea* (gamhar) wood. Three temperatures were used (140 °C, 160 °C and 180 °C) and two compaction rates (20 % and 40 %), applied for 30 minutes in a hot hydraulic press with final pressure of 2,5 MPa. Chemical changes, wettability and surface roughness of control and densified samples were investigated, as well as morphological changes. Densification partially degraded the hemicelluloses. Consequently, the wettability of the tangential surface of the densified wood decreased, with a more hydrophobic surface. Similarly, densification reduced surface roughness, especially when filtering was used for natural wood structures, with morphological changes on the surface of the densified samples. Densification with the highest temperature (180 °C) and 20 % compaction created the most hydrophobic surface (>90 °). In contrast, densification with the lowest temperature (140 °C) and compaction of 40 % provided the best results of the roughness parameters, with significant reductions, making it an applicable technique to minimize the roughness of wood in general and improve surface quality.

Keywords: Surface roughness, densification, hydrophobicity, thermos-mechanical treatment, wettability, wood chemistry, wood morphology.

Received: 02.02.2021

Accepted: 28.05.2024

Introduction

The application of heat and pressure together on the wood is called thermo mechanical densification. This promotes changes in material properties, and is an alternative for applications in lignocellulosic products by causing modifications of aesthetic and structural factors. The method consists of compacting the wood through pressing under heat, condensing the porous cells of the wood. This intensifies the internal friction between them, obtaining a denser cellular structure, which improves the characteristics of the wood (He *et al.* 2020, Carvalho *et al.* 2021, Tenorio *et al.* 2023).

Chemical and physical changes in the main constituents of wood surfaces reveal differences in its chemical structure, in particular changes in the OH groups of densified wood (Gonultas and Candan 2018, Li *et al.* 2022, Alqrinawi *et al.* 2024). The behavior of water on the wood surface is affected by chemical factors and surface irregularities, generating different shapes of water droplets, depending on the time of contact with the wood. The variation indicates the level of free energy at the surface of the material, which implies changes in wettability. This can be verified by measuring the contact angle between the surface and a liquid (Yuan and Lee 2013, Raabe *et al.* 2017).

Related to wettability is the intensity of peaks and valleys of the material plane. This parameter indicates how smooth or irregular the surface is, called roughness. For industrial applications, the precise characterization of the surface roughness is of significant importance, due to its considerable functional influence on the manufactured products (Whitehouse 2011).

Thermomechanical densification tends to leave the wood less porous and smoother (less surface roughness), thus modifying the activity of water on the surface. Wettability interferes with the contact relationships of wood with adhesives and coatings (Bekhta and Krystofiak 2016), therefore affecting the degree of adhesion and bonding of these materials.

Investigations of wettability and surface roughness have been performed involving different densification processes (Bekhta and Krystofiak 2016, Bekhta *et al.* 2018, Chu *et al.* 2019, Zao *et al.* 2020, Gao and Huang 2022, Gullo *et al.* 2023), with different results. Temperature, time and pressure act in the process, along with the compaction rate, which should be especially considered since it dictates the behavior as a function of the chemical and anatomical structure of wood of different species. Densification is considered an effective way to improve the mechanical properties of wood (Luan *et al.* 2022, Cabral *et al.* 2022), but to achieve good results, information is required about the optimal combinations of treatment parameters to improve the properties of specific woods (Schwarzkopf 2020, Cabral *et al.* 2022).

When the raw material comes from fast-growing species with low commercial interest, such as gamhar (*Gmelina arborea* Roxb.), there is a real possibility of enhancing the value of the product obtained in the process by achieving the desired functionality, thus increasing demand for the species to make high quality products.

We investigated the optimal conditions for thermomechanical densification of gamhar (*Gmelina arborea* Roxb.) wood as a function of temperature and compaction rate. The chemical, morphological, wettability and surface roughness parameters were determined of wood samples submitted to thermomechanical densification at 140 °C, 160 °C and 180 °C with 20 % and 40 % compaction rates.

Materials and methods

Samples of gamhar (*Gmelina arborea* Roxb.) wood, 25 years old, from stands planted in southern Brazil (25°34'17.8"S - 53°07'20.9"W), with dimensions of 25 mm x 100 mm x 2500 mm (thickness x width x length) and moisture content of $\cong 13$ % were used for thermomechanical densification. The samples were compacted in the perpendicular direction in a hot hydraulic press. The processing conditions were defined after pre-testing, in which internal wood temperatures of at least 100 °C were reached, with application of a pressure equivalent to 40% of the perpendicular compressive strength, to note the changes in properties.

Three temperatures (140 °C, 160 °C and 180 °C) and two compaction rates (20 % and 40 %) were applied to the treated samples for comparison with the control samples (Table 1). A 40 % compaction rate at 180 °C resulted in imperfections and defibration of the samples, thus not justifying further investigation of these parameters.

Table 1: Thermo mechanical densification treatments of gamhar (*Gmelina arborea* Roxb.) wood.

Treatments	Control	140 °C		160 °C		180 °C
	T0	T1	T2	T3	T4	T5
Compaction	-	20 %	40 %	20 %	40 %	20 %
Identification	Control	140 °C↓20 %	140 °C↓40 %	160 °C↓20 %	160 °C↓40 %	180 °C↓20 %

At the desired temperature, 10 samples per treatment were inserted into the press and a pressure ramp of 0,5 MPa per minute was applied until it reached 2,5 MPa \pm 0,3 MPa. After 30 minutes, the heating was discontinued and a pressure reduction ramp was applied at the same rate as the initial ramp until it reached 0,5 MPa. This condition was maintained for 240 minutes for internal temperature reduction (to 75 °C), tension relief and steam pressure, setting up post-treatment. Density, swelling, thickness and equilibrium moisture content of the samples were analyzed after 72 hours of immersion in water.

Changes in chemical constituents

Samples with thickness of 2 mm were examined by Fourier-transform infrared spectroscopy (FTIR) with attenuated total reflectance (ATR) to verify changes in the macromolecular chemical constituents of the wood surface. The spectra were obtained with an Alpha Bruker spectrometer and Alpha-P module (Karlsruhe, Germany), with diamond crystal, in the spectral range of 400 cm^{-1} to 4000 cm^{-1} , resolution of 4 cm^{-1} and 32 scans.

Wettability analysis

Three drops of deionized water with a volume of $5\text{ }\mu\text{L}$ were deposited on the abaxial and adaxial surfaces of the material. The apparent contact angle (CA) was measured at predetermined times (5 seconds, 15 seconds and 30 seconds).

Surface roughness determination

The surface roughness of the material was analyzed with a non-contact mode 3D optical profilometer (white light interferometer, Talysurf CCI, Taylor Hobson). The parameters S_a (mean roughness), S_q (mean quadratic roughness) and S_z (maximum surface height)

were determined at three points on the abaxial surface and three points on the adaxial surface of the samples, corresponding to a reading field of 0,75 mm², according to ISO 25178 (2013).

The parameters Spk (reduced peak height), Sk (depth of core roughness) and Svk (reduced valley depth) were determined according to the EUR 15178N (1993). The sampling length (cutoff) was set at 0,025 mm and a Gaussian regression filter was applied for data analysis.

Surface morphology

The morphology of the radial, tangential and transversal sections of the control and densified samples were analyzed by scanning electron microscopy (SEM). The samples were dried, cut and metallized (sputter coated) with a thin layer of gold. Under low vacuum with electron beam intensity of 15kV, high resolution images at different magnifications were acquired in a JEOL JSM 6360-LV microscope.

Statistical analysis

The data were tabulated in electronic spreadsheets and analyzed for variance homogeneity (Bartlett and Hartley tests) and data normality (Kolmogorov-Smirnov test). The parameters of apparent contact angle and roughness were analyzed by analysis of

variance ($p \leq 0,05$), and significant differences were verified with the Tukey test ($p \leq 0,05$) to compare means.

Results and discussion

The natural density of the material was 450 kg/m^3 . The highest density values were obtained for samples subjected to 40% compaction (T2 and T4), reaching 680 kg/m^3 and 670 kg/m^3 , respectively. For T3 and T5, the apparent densities were 540 kg/m^3 and 560 kg/m^3 . The increase in density occurs as a result of the compaction (Unsal *et al.* 2011, Arruda and Del Menezzi 2013, Cabral *et al.* 2022). Compaction directly influences dimensional stability, with a tendency for swelling in samples with higher compression rates (Unsal *et al.* 2011, Cai *et al.* 2012).

In this study, the maximum thickness swelling after 72 hours of immersion in water was 8,76 % (T2), less than 10 %, due to the relief of internal tension and residual stress of the cells, resulting from post-treatment. The densification obtained by the process was partially lost when the material came into contact with water, so it was not possible to completely eliminate the effect of initial shape memory. Therefore, viscoelastic tensions were partially alleviated by the solidification of the lignin-hemicellulose matrix (Scharf *et al.* 2023) before release of the compression load (Scharf *et al.* 2023). Densification reduced the equilibrium moisture content (T0=13 % / T1=10,93 / T2=10,34 / T3=9,27 / T4=9,46 / T5=7,62). The lower equilibrium moisture content of densified wood is due to the smaller amounts of water adsorbed by the cell wall after treatment, in turn attributed

to the increase in the wood's crystallinity index due to the reduction in the amorphous portion of the hemicelluloses (Navi and Sandberg 2012, Sandberg *et al.* 2023).

Changes in chemical constituents

The chemical changes observed after the application of thermomechanical densification were identified by peak intensities, especially in the range between 1800 cm^{-1} and 800 cm^{-1} , known as the wood identity region (Figure 1).

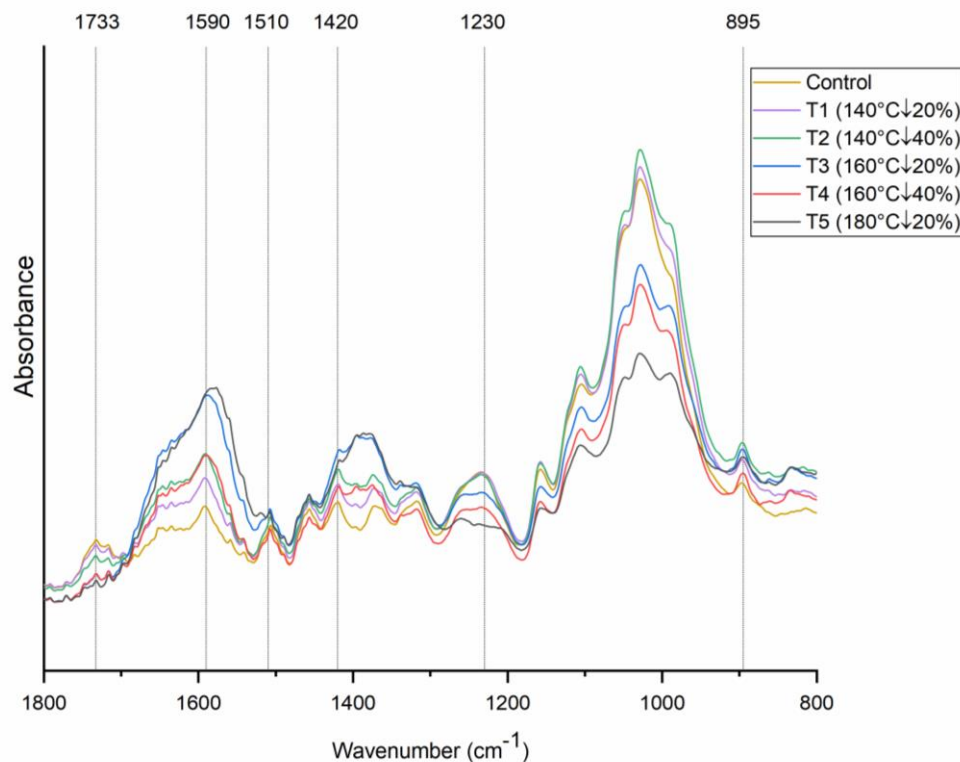


Figure 1: FTIR-ATR spectra for the control and densified gamhar (*Gmelina arborea* Roxb.) wood samples.

In the region of 1733 cm^{-1} it is possible to notice the lower intensity of peaks as a function of the increase in densification temperature. This change is attributed to the elongation of

carbonyl groups (C=O) in hemicelluloses, lignin and extractives (Fu *et al.* 2019, Alqrinawi *et al.* 2024). Decreasing intensity peaks suggest the cleavage of ester groups associated with the decomposition of hemicellulose polysaccharides (Inari *et al.* 2006), with the lowest magnitude occurring in treatment T5 (180 °C↓20 %).

Widening of the densification peaks along with a small displacement to a longer wavelength can be seen near 1590 cm⁻¹ and 1510 cm⁻¹, associated with the aromatic skeletal vibration of lignin (Guo *et al.* 2015, Bao *et al.* 2018), which can be caused by the division of the aliphatic lateral chain in the lignin reactions (Windeisen and Wegener 2008, Bao *et al.* 2018).

In the region 1230 cm⁻¹, corresponding to the C=O absorption band (Diouf *et al.* 2011), T5 (180 °C↓20 %), T4 (160 °C↓40 %) and T3 (160 °C↓20 %), treatments with higher temperatures, differed from the others, with a reduction in peak intensity. This can be attributed to the degradation of hemicelluloses, gradually intensified from the control to T5 (180 °C↓20 %). Peak intensities in the regions 1420 cm⁻¹ and 895 cm⁻¹ were observed for the densified samples. These changes are due to the flexion vibration, attributed to cellulose (Diouf *et al.* 2011), which indicates a relative increase of cellulose after densification.

The analysis indicated a certain degree of degradation of the chemical functional groups, in particular the hemicelluloses. This change reflects the more hydrophobic behavior of the tangential surface of the densified wood in relation to the control.

Wettability associated with densification

The densification changed the tangential face of the wood, from hydrophilic to hydrophobic, with contact angles greater than 90° , especially after 5 seconds of exposure. On the radial face, the behavior did not follow the same trend, which is explained by the non-contact of this face with the heated press. The time sequence changes the shape of the drop and consequently the apparent contact angle (Figure 2).

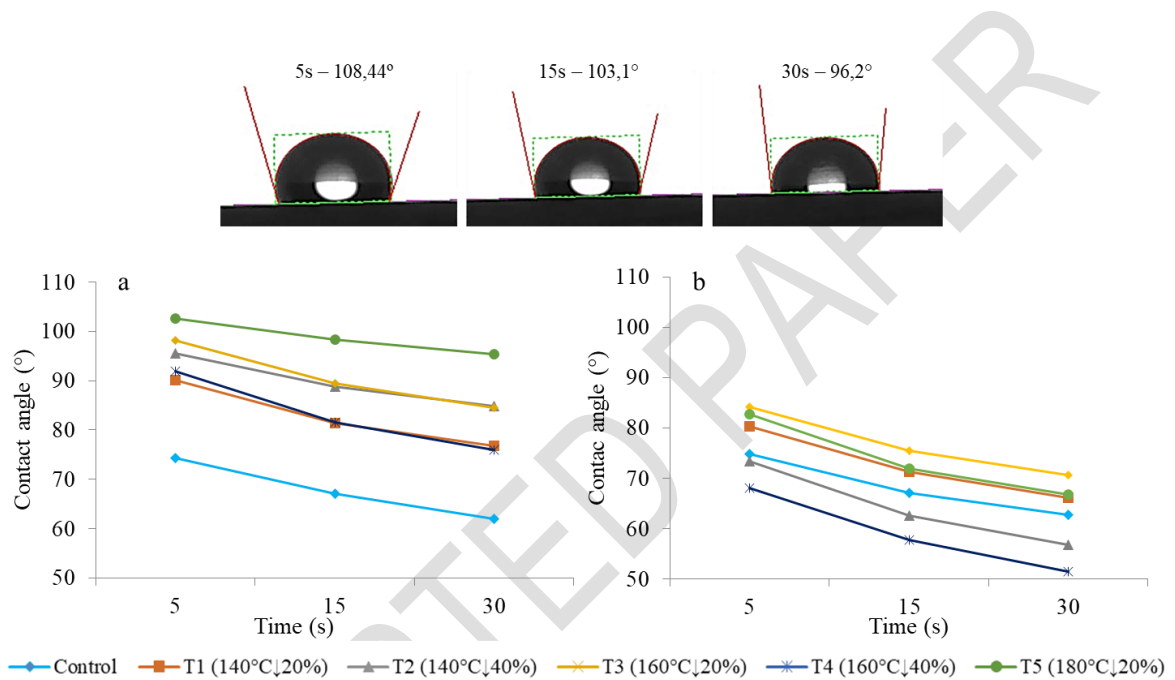


Figure 2: Behavior of the contact angle in control and densified gamhar (*Gmelina arborea* Roxb.) wood samples.
a) = Tangential face; b) = Radial face.

The control sample had the smallest apparent contact angle, so it was more wettable on the tangential face. This indicates that densification caused stronger interaction of physical and chemical factors that modified the surface. Such phenomena, such as partial closure of the pores and reduction of the hydroxyl groups of the tangential surface, caused a surface sealing effect, making it more hydrophobic (Figure 3).

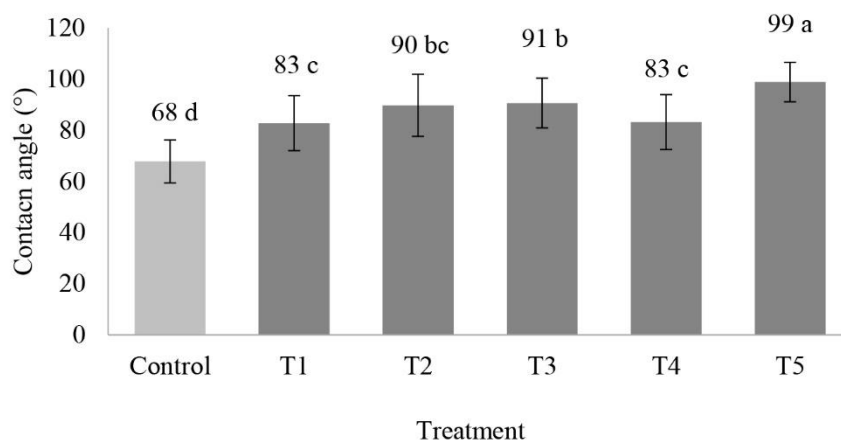


Figure 3: Apparent contact angle on tangential surface in control and densified gamhar (*Gmelina arborea* Roxb.) wood samples. T1 = 140 °C↓20 %; T2 = 140 °C↓40 %; T3 = 160 °C↓20 %; T4 = 160 °C↓40 %; T5 = 180 °C↓20 %. The bars on the columns indicate the standard deviation.

The degradation of hemicelluloses and relative increase of cellulose, previously observed in the spectroscopic analysis, corroborates the greater contact angle of the densified samples, especially T2 (140 °C↓40 %), T3 (160 °C↓20 %) and T5 (180 °C↓20 %).

The application of heat causes the migration of the extractives to the wood surface, reorganization of the lignocellulosic polymeric components and plasticization of the lignin, altering the hydrophilic properties of the wood (Hakkou *et al.* 2005, Metsä-Kortelainen and Viitanen 2012, Santos *et al.* 2012). These factors favor the reduction of wettability.

In the radial section of the samples, which were not in direct contact with the heated plates of the press, different behavior from that observed in the tangential section can be observed (Figure 4), and there is no logical sequence.

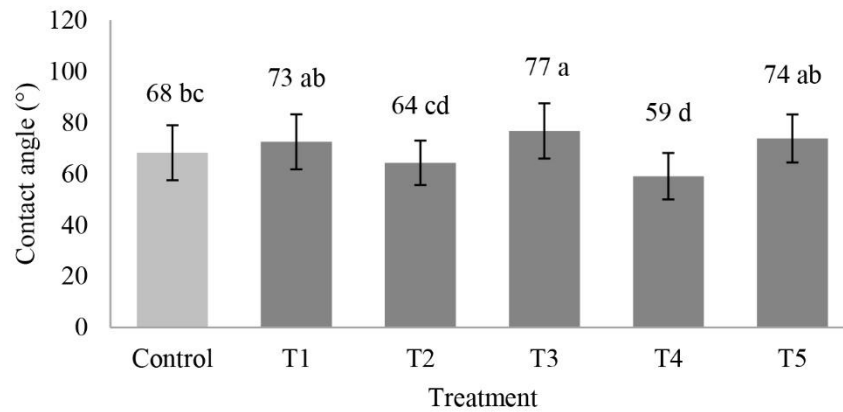


Figure 4: Apparent contact angle of radial surface in control and densified gamhar (*Gmelina arborea* Roxb.) wood samples. T1 = 140 °C↓20 %; T2 = 140 °C↓40 %; T3 = 160 °C↓20 %; T4 = 160 °C↓40 %; T5 = 180 °C↓20 %. The bars on the columns indicate the standard deviation.

The behavior observed in the radial and tangential sections was the same as the control. For the other treatments, the apparent contact angle in the radial direction was smaller than on the tangential surface. From a practical point of view, this behavior allows the application of densified parts in the production of laterally bonded articles, since it does not impair the bonding of the radial section.

Effect of densification on wood roughness

The densification altered the surface roughness, observed by the representative topography of the samples (Figure 5).

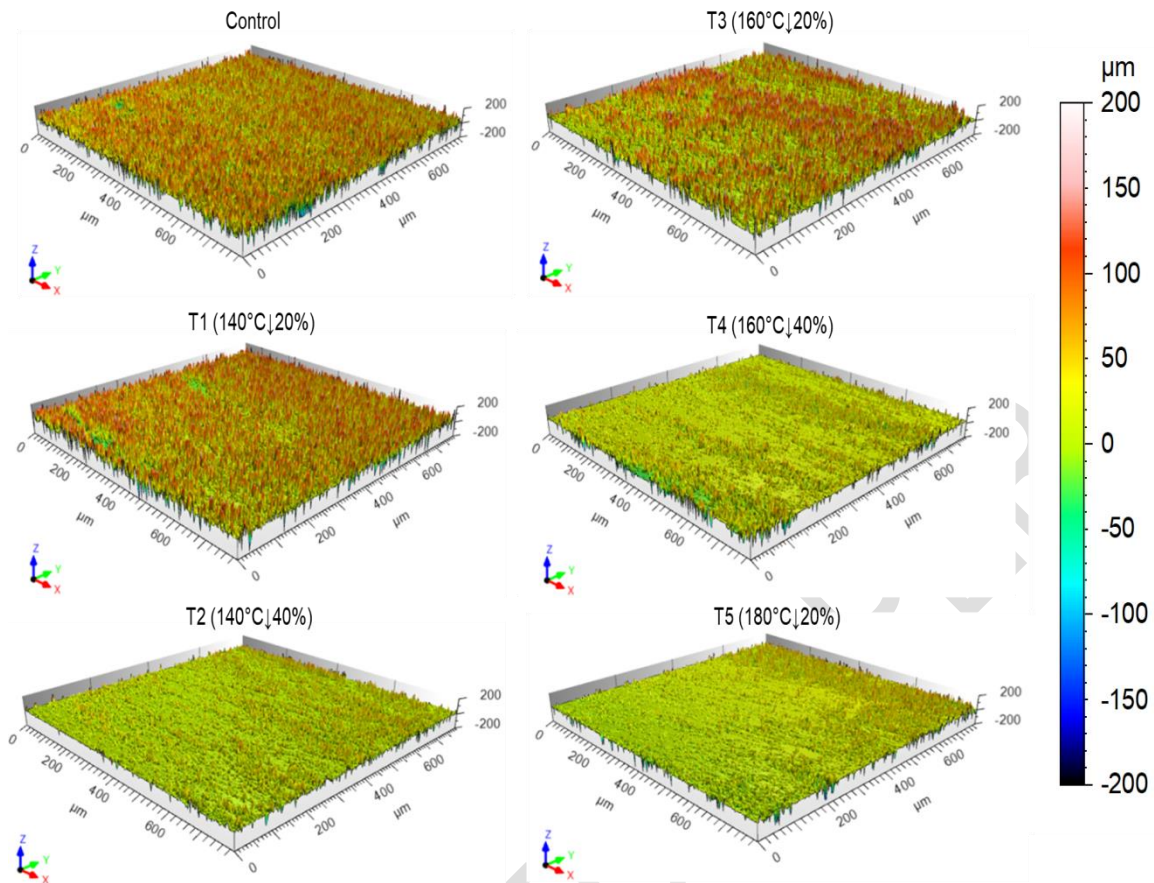


Figure 5: 3D surface roughness of control and densified gamhar (*Gmelina arborea* Roxb.) wood samples.

The change in the topography of the material was more intense with T2 (140 °C ↓ 40 %), which caused a significant reduction of all parameters in relation to the control. The decrease was 60 % for the mean roughness (Sa), 50,18 % for the mean quadratic roughness (Sq), and 30,98 % for the total roughness (Sz), with statistical similarity to T5 (Table 2).

Table 2: 3D surface roughness parameters of the control and densified of gamhar (*Gmelina arborea* Roxb.) wood samples.

Treatment	Sa (μm)	Sq (μm)	Sz (μm)
Control	7,25 (2,08) d	10,96 (2,67) d	116,18 (19,35) c
T1 (140 °C↓20 %)	5,72 (0,83) c	10,42 (1,01) d	148,54 (7,93) d
T2 (140 °C↓40 %)	2,90 (0,98) a	5,46 (1,47) a	80,18 (13,13) a
T3 (160 °C↓20 %)	5,47 (0,82) c	10,01 (1,04) cd	146,55 (11,18) d
T4 (160 °C↓40 %)	4,66 (1,09) bc	8,35 (1,77) bc	105,64 (16,43) bc
T5 (180 °C↓20 %)	3,83 (0,92) ab	6,89 (1,24) ab	91,81 (8,68) ab
F value	19,37	21,27	52,79

Sa = mean roughness; Sq = mean square roughness; Sz = maximum surface height, difference between the highest peak and the deepest valley. Significant at 95 % confidence level; Mean values followed by the same letter have no statistical difference at 5 % probability of error. Values in parentheses correspond to the standard deviation.

The average roughness obtained in *Corymbia* and *Eucalyptus* machined wood floors was between 2,34 μm and 2,69 μm , with combinations of forward speed and cutting speed (Silva *et al.* 2016). In a study of sanding and application of surface sealer on balata blanc (*Micropholis venulosa* (Mart. & Eichler)), mean roughness values between 3,44 μm and 9,96 μm were reported (Raabe *et al.* 2017). The similarities of those values with the ones found by us indicate that thermomechanical densification minimizes roughness, comparable to methods already consolidated industrially. Material losses due to sanding and planning processes are avoided with the application of densification, with lower quantity of byproducts generated.

For the mean roughness (Sa), the densification showed significantly lower values than the control. The mean quadratic roughness (Sq), T1 (140 °C↓20 %) and T3 (160 °C↓20 %) did not differ from the control. For the maximum surface height (Sz) and total roughness, T1 and T3 presented values above the control, i.e., they presented greater differences between the highest peak and the deepest valley in relation to the control sample.

This fact was not expected, because with the densification, roughness parameters below the control were desired. This may have occurred due to the difference in the size and distribution of the sample pores, thus altering the surface texture of the wood.

This occurrence is explained by the data in Table 3, where the control has roughness parameters (SpK, Sk and SvK) statistically higher than or equal to the densified samples. These parameters are based on the Abbott curve, a filtering technique used to discern the natural irregularities of the material, such as the anatomical parameters of the intrinsic roughness of the treatments applied (Gurau *et al.* 2004, Sandak and Negri 2005).

Table 3: 3D surface roughness parameters of the control and densified gamhar (*Gmelina arborea* Roxb.) wood samples.

Treatment	SpK (µm)	SK (µm)	SvK (µm)
Control	18,03 (3,82) d	12,29 (5,06) c	19,60 (4,38) c
T1 (140 °C↓20 %)	17,06 (2,04) cd	5,52 (2,38) b	19,53 (2,59) c
T2 (140 °C↓40 %)	8,92 (2,53) a	1,88 (1,33) a	10,70 (3,38) a
T3 (160 °C↓20 %)	16,52 (1,98) cd	5,03 (2,40) ab	18,58 (2,52) c
T4 (160 °C↓40 %)	14,04 (3,58) bc	3,27 (1,53) ab	16,51 (4,36) bc
T5 (180 °C↓20 %)	11,40 (1,99) ab	2,98 (1,93) ab	13,60 (3,41) ab
F value	20,08	22,48	12,62

Spk (reduced peak height), Sk (depth of core roughness) and SvK (reduced valley depth). Significant at 95 % confidence level; Mean values followed by the same letter have no statistical difference at 5 % probability of error. Values in parentheses correspond to the standard deviation.

Since characteristics of wood such as the shape of anatomical structures (Cademartori *et al.* 2017) are modified, especially elimination of the vessels responsible for surface valleys, densification reduces the roughness parameters. The reduction of T2 (140 °C↓40 %) and T5 (180 °C↓20 %), with mean values below those of the control and samples with other densifications, is noteworthy. These had a smoother surface, with greater aesthetic appeal for industrial applications.

An example is the use of wood without finishes or for the application of paints, varnishes and other coatings, where smoother surfaces of roofing and siding mean lower consumption (Sandak and Negri 2005, Bekhta *et al.* 2014). From the industrial and economic points of view, our results indicate it is preferable to apply a treatment with the

lowest temperature (140 °C) and highest compaction (40 %), since there is less energy expenditure to obtain a reduction of the roughness parameters.

By applying a filter to eliminate the anatomical influence of wood, we observed that the thermomechanical densification reduced all indicators of surface roughness, which is desirable in many applications by favoring lower wettability.

Scanning electron microscopy

In transversal morphology, a change in the shape of the vessels was observed, changing from an oval shape in the control to a flattened shape with the application of densification, reducing the volume of the pores (Figure 6). This behavior was also observed in other studies of densified wood (Dömény *et al.* 2018, Wu *et al.* 2020).

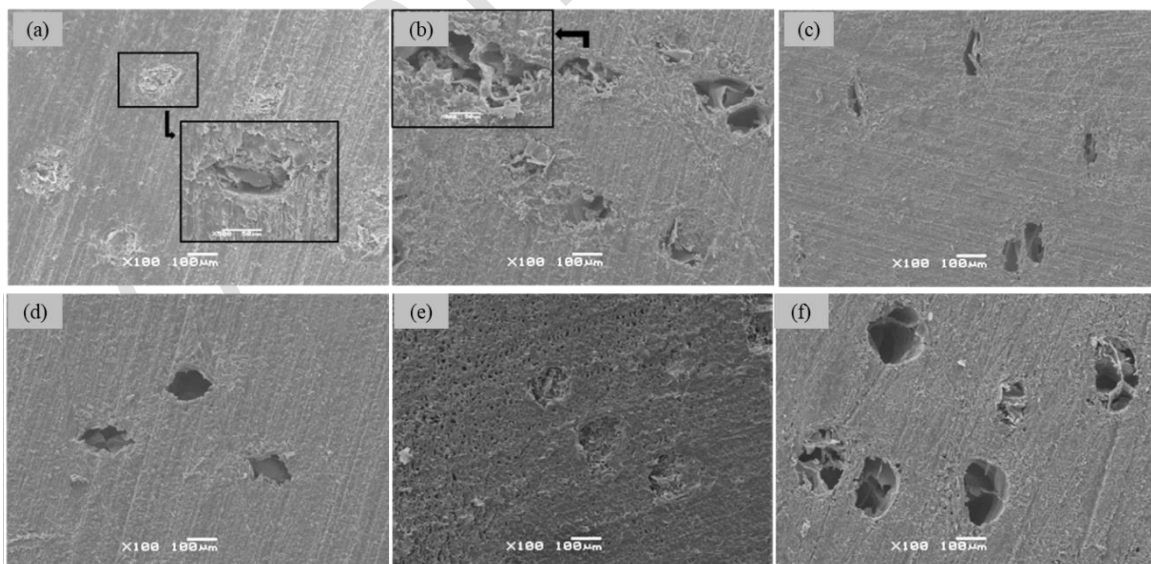


Figure 6: Scanning electron microscopic images of the transversal face of gamhar (*Gmelina arborea* Roxb.).

(a) (T1 = 140 °C ↓ 20 %); b) (T2 = 140 °C ↓ 40 %); c) (T3 = 160 °C ↓ 20 %); d) (T4 = 160 °C ↓ 40 %); e) (T5 = 180 °C ↓ 20 %); f) (Control).

On the tangential face, there were distinctions between the rays, vessels and fibers of the treated samples and control sample. The densified samples had smoother surfaces due to the crushing of these elements (Figure 7), reducing the wettability of this face.

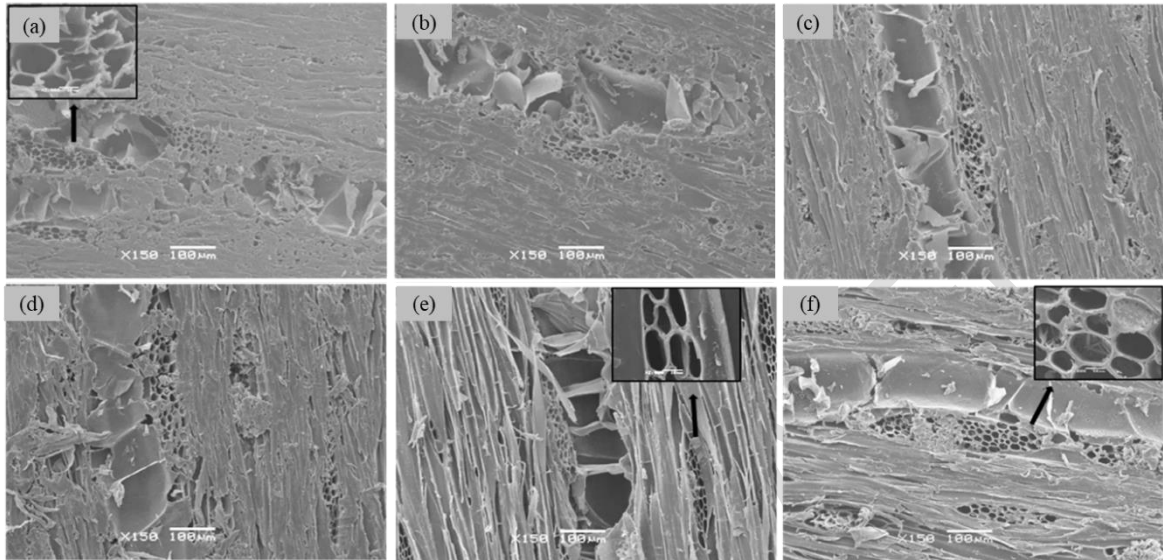


Figure 7: Scanning electron microscopic images of the tangential face of gamhar (*Gmelina arborea* Roxb.).

(a) (T1 = 140 °C↓20 %); (b) (T2 = 140 °C↓40 %); (c) (T3 = 160 °C↓20 %); (d) (T4 = 160 °C↓40 %); (e) (T5 = 180 °C↓20 %); (f) (Control).

For T5 (180 °C↓20 %), the crushing aspect is not as visible, but tissue defibration can be noted in the detail (Figure 7e). This fact was observed in the treatment with the highest temperature, associated with the degradation of the hemicelluloses that envelope the fibrils, leading to their dismemberment. Regarding ray cells, in the control there was no alteration of the cell walls, unlike observed in densified samples, where there were ruptures of the cell walls associated with superficial flattening (Figure 7a).

Like on the tangential face, there was alteration of fibers on the radial face (Figure 8). In the control samples, the fibers had a well-defined shape, with distribution parallel to each other along the wood.

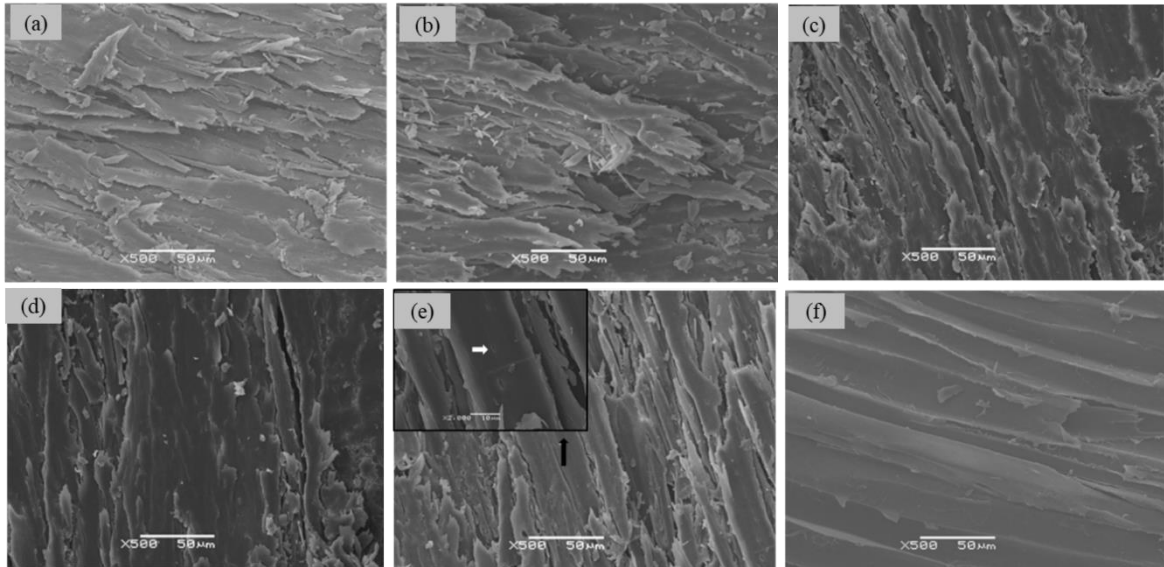


Figure 8: Scanning electron microscopic images of the radial face of gamhar (*Gmelina arborea* Roxb.).

(a) (T1 = 140 °C ↓20 %); (b) (T2 = 140 °C ↓40 %); (c) (T3 = 160 °C ↓20 %); (d) (T4 = 160 °C ↓40 %); (e) (T5 = 180 °C ↓20 %); (f) (Control).

In densified wood, the structure has an irregular shape, similar to that caused by fibrillar crushing, making structural distinction difficult, with cracks (Figure 8e). This change is due to the heat applied, which limits the application of this process with a temperature of 180 °C or above.

Conclusions

This study investigated the surface effects on the chemistry, wettability and roughness of *Gmelina arborea* wood specimens submitted to thermomechanical densification. In general, the densification degraded the hemicelluloses present on the wood surface structure, reduced the wettability of the tangential face and the surface roughness.

The densification with the lowest temperature (140 °C) and compaction of 40 %, produced the lowest surface roughness rates. The densification with the highest temperature (180 °C) and compaction of 20 % caused a greater contact angle of the tangential face, with values above 100 °. This caused the naturally hydrophilic surface of *Gmelina arborea* wood to present a hydrophobic character, enabling applications in situations that require water repellence.

Changes in the morphology of the densified samples coincided with improved surface quality of the wood. The densification process can thus be an alternative to increase the value of wood from species with low commercial interest, by reducing wettability and surface roughness in comparison with natural wood.

Author contributions

D. E. C.: Conceptualization, investigation, methodology, project administration, formal analysis, writing - original draft. M. P. R.: Supervision, validation. R. J. K.: Writing - original draft, visualization. P. H. G. C.: Formal analysis, writing - review & editing

Acknowledgements

This work was supported by the National Council for Scientific and Technological Development (CNPq- process 154362/2016-6).

References:

- Alqrinawi, H.; Ahmed, B.; Wu, Q.; Lin, H.; Kameshwar, S.; Shayan, M. 2024.** Effect of partial delignification and densification on chemical, morphological, and mechanical properties of wood: Structural property evolution. *Industrial Crops and Products* 213: e118430. <https://doi.org/10.1016/j.indcrop.2024.118430>
- Arruda, L.M.; Del Menezzi, C.H.S. 2013.** Effect of thermomechanical treatment on physical properties of wood veneers. *International Wood Products Journal* 4(4): 217-224. <https://doi.org/10.1179/2042645312Y.0000000022>
- Bao, M.; Huang, X.; Jiang, M.; Li, N.; Yu, Y.; Yu, W. 2018.** Study on the changes in surface characteristics of *Populus tomentosa* due to thermo-hydro-process. *Journal of Wood Science* 64: 264-278. <https://doi.org/10.1007/s10086-018-1697-9>

Bekhta, P.; Krystofiak, T. 2016. The influence of short-term thermo-mechanical densification on the surface wettability of wood veneers. *Maderas. Ciencia y Tecnología* 18(1): 79-90. <https://doi.org/10.4067/S0718-221X2016005000008>

Bekhta, P.; Krystofiak, T.; Proszyk, S.; Lis, B. 2018. Surface gloss of lacquered medium density fibreboard panels veneered with thermally compressed birch wood. *Progress in Organic Coatings* 117: 10-19. <https://doi.org/10.1016/j.porgcoat.2017.12.020>

Bekhta, P.; Proszyk, S.; Krystofiak, T.; Mamonova, M.; Pinkowski, G.; Lis, B. 2014. Effect of thermomechanical densification on surface roughness of wood veneers. *Wood Material Science & Engineering* 9(4): 233-245. <https://doi.org/10.1080/17480272.2014.923042>

Cabral, J.P.; Kafle, B.; Subhani, M.; Reiner, J.; Ashraf, M. 2022. Densification of timber: a review on the process, material properties, and application. *Journal of Wood Science* 68: e20. <https://doi.org/10.1186/s10086-022-02028-3>

Cademartori, P.H.G.; Stafford, L.; Blanchet, P.; Magalhães, W.L.E.; Muniz, G.I.B. 2017. Enhancing the water repellency of wood surfaces by atmospheric pressure cold plasma deposition of fluorocarbon film. *RSC Advances* 46(7): 29159-29169. <https://doi.org/10.1039/C7RA03334F>

Cai, J.B.; Ding, T.; Yang, L. 2012. Dimensional stability of poplar wood after densification combined with heat treatment. *Applied Mechanics and Materials* (152-154): 112-116. <https://doi.org/10.4028/www.scientific.net/AMM.152-154.112>

Carvalho, D.E.; Rocha, M.P.; Klitzke, R.J.; Cademartori, P.H.G. 2021. Colour changes and equilibrium moisture content on thermomechanical densified wood. *Anais da Academia Brasileira de Ciências* 93(4). <https://doi.org/10.1590/0001-3765202120200109>

Chu, D.; Mu, J.; Avramidis, S.; Rahimi, S.; Liu, S.; Lai, Z. 2019. Functionalized Surface Layer on Poplar Wood Fabricated by Fire Retardant and Thermal Densification. Part 2: Dynamic Wettability and Bonding Strength. *Forests* 10(11): e982. <https://www.mdpi.com/1999-4907/10/11/982>

Diouf, P.N.; Stevanovic, T.; Cloutier, A.; Fang, C.H.; Blanchet, P.; Koubaa, A.; Mariotti, N. 2011. Effects of thermo-hygro-mechanical densification on the surface characteristics of trembling aspen and hybrid poplar wood veneers. *Applied Surface Science* 257(8): 3558-3564. <https://doi.org/10.1016/j.apsusc.2010.11.074>

Dömény, J.; Čermák, P.; Koiš, V.; Tippner, J.; Rousek, R. 2018. Density profile and microstructural analysis of densified beech wood (*Fagus sylvatica* L.) plasticized by microwave treatment. *European Journal of Wood and Wood Products* 76(7): 105-111. <https://doi.org/10.1007/s00107-017-1173-z>

ER. 1993. The development of methods for the characterisation of roughness in three dimensions. Commission of the European Communities, EUR 15178N EM, Butterworth-Heinemann Elsevier Ltd, Oxford, United Kingdom.

Fu, Q.; Cloutier, A.; Laghdar, A.; Stevanovic, T. 2019. Surface Chemical Changes of Sugar Maple Wood Induced by Thermo-Hygro-mechanical (THM) Treatment. *Materials* 12(12). e1946. <https://doi.org/10.3390/ma12121946>

Gao, Z.; Huang, R. 2022. Effects of Pressurized Superheated Steam Treatment on Dimensional Stability and Its Mechanisms in Surface-Compressed Wood. *Forests* 13(8): e1230. <https://doi.org/10.3390/f13081230>

Gullo, F.; Marangon A.; Croce, A.; Gatti, G.; Aceto, M. 2023. From Natural Woods to High Density Materials: An Ecofriendly Approach. *Sustainability* 15(3): e2055. <https://doi.org/10.3390/su15032055>

Gonultas, O.; Candan, Z. 2018. Chemical characterization and ftir spectroscopy of thermally compressed eucalyptus wood panels. *Maderas. Ciencia y Tecnología* 20(3): 431-442. <https://doi.org/10.4067/S0718-221X2018005031301>

Guo, J.; Song, K.; Salmén, L.; Yin, Y. 2015. Changes of wood cell walls in response to hygro-mechanical steam treatment. *Carbohydrate Polymers* 115: 207-214. <https://doi.org/10.1016/j.carbpol.2014.08.040>

Gurau, L.; Mansfield-Williams, H.; Irle, M. 2005. Processing roughness of sanded wood surfaces. *Holz Roh Werkst* 63: 43-52. <https://doi.org/10.1007/s00107-004-0524-8>

Hakkou, M.; Petrissans, M.; El Bakali, I.; Gerardin, P.; Zoulalian, A. 2005. Wettability changes and mass loss during heat treatment of wood. *Holzforchung* 59: 35-37. <https://doi.org/10.1515/HF.2005.006>

He, S.; Chen, C.; Li, T.; Song, J.; Zhao, X.; Kuang, Y.; Liu, Y.; Pei, Y.; Hitz, E.; Kong, W.; Gan, W.; Yang, B.; Yang, R.; Hu, L. 2020. An energy-efficient, wood-derived structural material enabled by pore structure engineering towards building efficiency. *Small Methods* 4(1): e1900747. <https://doi.org/10.1002/smt.201900747>

Inari, G.N.; Petrissans, M.; Lambert, J.; Ehrhardt, J.; Gérardin, P. 2006. XPS characterization of wood chemical composition after heat-treatment. *Surface and Interface Analysis* 38(10): 1336-1342. <https://doi.org/10.1002/sia.2455>

ISO. 2013. Geometrical Product Specifications (GPS). ISO 25178-3, Surface texture: Areal - Part 3.

Li, K.; Zhao, L.; Ren, J.; He, B. 2022. Interpretation of strengthening mechanism of densified wood from supramolecular structures. *Molecules* 27(13): e4167. <https://doi.org/10.3390/molecules27134167>

Luan, Y.; Fang, C.H.; Ma, Y.F.; Fei, B.H. 2022. Wood mechanical densification: a review on processing. *Materials and Manufacturing Processes* 37(4): 359-371. <https://doi.org/10.1080/10426914.2021.2016816>

Metsä-Kortelainen, S.; Viitanen, H. 2012. Wettability of sapwood and heartwood of thermally modified Norway spruce and Scots pine. *European Journal of Wood and Wood Products* 70(1-3):135-139. <https://doi.org/10.1007/s00107-011-0523-5>

Navi, P.; Sandberg, D. 2012. Thermo-Hydro-Mechanical Processing of Wood. EPEL Press, Lausanne, Switzerland. <https://www.epflpress.org/produit/507/9782940222411/thermo-hydro-mechanical-processing-of-wood>

Raabe, J.; Del Menezzi, C.; Goncalvez, J. 2017. Avaliação da Superfície de Lâminas Decorativas de Curupixá (*Micropholis venulosa* Mart. Eichler). *Floresta e Ambiente* 24: e20150054. <https://doi.org/10.1590/2179-8087.005415>

Sandak, J.; Negri, M. 2005. Wood surface roughness- What is it? - In: Proceedings of the 17th International Wood Machining Seminar (IWMS 17). Rosenheim, Germany. https://www.researchgate.net/publication/267805159_Wood_surface_roughness_-_what_is_it

Sandberg, D.; Eggert, O.; Haider, A.; Kamke, F.; Wagenführ, A. 2023. Forming, Densification and Molding. In: Springer Handbook of Wood Science and Technology. Cham: Springer International Publishing. http://dx.doi.org/10.1007/978-3-030-81315-4_18

Santos, C.M.T.; Del Menezzi, C.H.; Souza, M.R. 2012. Properties of thermo-mechanically treated wood from *Pinus caribaea* var. *hondurensis*. *BioResources* 7(2): 1850-1865. <https://doi.org/10.15376/biores.7.2.1850-1865>

Scharf, A.; Neyses, B.; Sandberg, D. 2023. Continuous densification of wood with a belt press: the process and properties of the surface-densified wood. *Wood Material*

Science & Engineering 18(4): 1573-1586.
<https://doi.org/10.1080/17480272.2023.2216660>

Scharf, A.; Lemoine, A.; Neyses, B.; Sandberg, D. 2023. The effect of the growth ring orientation on spring-back and set-recovery in surface-densified wood. *Holzforschung* 77 (6): 394-406. <https://doi.org/10.1515/hf-2023-0004>

Schwarzkopf, M. 2020. Densified wood impregnated with phenol resin for reduced set-recovery. *Wood Material Science & Engineering* 16(1): 35-41.
<https://doi.org/10.1080/17480272.2020.1729236>

Silva, F.A.V.; Silva, J.R.M.; Moulin, J.C.; Andrade, A.C.A.; Nobre, J.R.C.; Castro, J.P. 2016. Qualidade da superfície usinada em pisos de madeira de *Corymbia* e *Eucalyptus*. *Floresta* 46(3):397-403. <https://doi.org/10.5380/ufv.v46i3.43936>

Tenorio, C.; Moya, R.; Starbird-Perez, R. 2023. Effect of steaming and furfuryl alcohol impregnation pre-treatments on the spring back, set recovery and thermal degradation of densified wood of three tropical hardwood species. *European Journal of Wood and Wood Products* 81(2): 467-480.<https://doi.org/10.1007/s00107-022-01890-8>

Unsal, O.; Candan, Z.; Buyuksari, U.; Korkut, S.; Chang, Y.S.; Yeo, H. 2011. Effect of Thermal Compression Treatment on the Surface Hardness, Vertical Density Profile and Thickness Swelling of *Eucalyptus* Wood Boards by Hot-pressing. *Journal of the Korean Wood Science and Technology* 39(2): 48-155.
<https://doi.org/10.5658/WOOD.2011.39.2.148>

Whitehouse, D.J. 2011. *Handbook of Surface and Nanometrology*. 2nd Edition, CRC Press, Taylor & Francis: New York, United States of America.

Windeisen, E.; Wegener, G. 2008. Behaviour of lignin during thermal treatments of wood. *Industrial Crops and Products* 27(2): 157-162.
<https://doi.org/10.1016/j.indcrop.2007.07.015>

Wu, J.; Fan, Q.; Wang, Q.; Guo, Q.; Tu, D.; Chen, C.; Xiao, Y.; Ou, R. 2020. Improved performance of poplar wood by an environmentally-friendly process combining surface impregnation of a reactive waterborne acrylic resin and unilateral surface densification. *Journal of Cleaner Production* 261(1): e121022.
<https://doi.org/10.1016/j.jclepro.2020.121022>

Yuan, Y.; Lee, T.R. 2013. Contact angle and wetting properties. In: Bracco G, Holst B, editors. *Surface sciences techniques*. Springer-Verlag Berlin Heidelberg: New York, United States of America. <https://doi.org/10.1007/978-3-642-34243-1>

Zao, Y.; Qu, D.; Yu, T.; Xie, X.; He, C.; Ge, D.; Yang, L. 2020. Frost-resistant high-performance wood via synergetic building of omni-surface hydrophobicity. *Chemical Engineering Journal* 385: e123860. <https://doi.org/10.1016/j.cej.2019.123860>